COO-3077-52
MF-78

Courant Institute of
Mathematical Sciences

Magneto-Fluid Dynamics Division

Equilibria and Adiabatic Compression of Free Boundary Belt Pinches

A. Kadish and D. C. Stevens

AEC Research and Development Report

Nuclear Fusion
May 1974

New York University

UNCLASSIFIED

New York University
Courant Institute of Mathematical Sciences
Magneto-Fluid Dynamics Division

MF-78

COO-3077-52

EQUILIBRIA AND ADIABATIC COMPRESSION OF FREE BOUNDARY BELT PINCHES

A. Kadish and D.C. Stevens

May 1974

This work was supported by the U.S. Atomic Energy Commission under Contract No. AT(11-1) 3077.

UNCLASSIFIED

Abstract

The plasma shape and location of a sharp boundary belt pinch is determined by the dimensions of the surrounding conducting shell and by thermodynamic parameters. It is shown that, except for simple scaling, there exists a one-parameter family of equilibria. The plasma shape is uniquely determined by initial parameters and wall current. The variation of the plasma shape during an adiabatic compression is calculated as are plasma current, temperature, field strength, etc. As the compression ratio of the plasma is increased beyond two, the ratio of plasma height/width decreases to unity. For high compression ratios, the column cross-section becomes circular. Explicit solutions are obtained by conformal mapping.

Table of Contents

Section | Page
I. Introduction 1
II. The Free Boundary Problem 4
III. Asymptotics 9
IV. Adiabatic Compression 16
Acknowledgment 20
Appendix 21
References 24
Figures 25

I. Introduction

The desire for stable toroidal plasma equilibria has led to studies of plasma configurations with non-circular toroidal cross-sections.[1] Many of the efforts to determine equilibria for such configurations have been numerical investigations which assume a sharp boundary toroidal plasma, supported in equilibrium by a vacuum magnetic field. These calculations, which consider a variety of plasma current density distributions offer some surprising results. For example, plasma compression ratio limitations of the order of two, for highly non-circular plasmas, have been observed.[2,3] This limitation may be attributed to the lack of circular symmetry of the plasma cross-section. In determining such limitations, the aspect ratio is less important than the ratio of dimensions of the cross-section of the outer boundary of the torus.

In this paper, we present an analysis of configurations in which all the current in a uniform plasma column flows in the interface between the plasma column and the vacuum magnetic field which supports it in equilibrium. Numerical studies indicate that this configuration offers maximal compression ratios for a belt pinch column. We simplify our problem by neglecting toroidal curvature effects. That is, we replace the toroidal configuration, assumed to have a perfectly conducting closed toroidal shell of rectangular cross-section (see Fig.1), by a straight configuration. The toroidal axis of symmetry is replaced by a plane of symmetry. The closed toroidal outer boundary is replaced by two perfectly conducting straight sections symmetrically located on opposite sides of the plane of symmetry (see Fig. 2). These straight sections carry oppositely directed "toroidal" current.

Toroidal current in the outer boundary induces a toroidal sheath current at the plasma boundary which in turn induces a poloidal vacuum field in the region between the plasma column and the outer boundary. An increase in this field alters the pressure and shape of the column in order to provide local pressure balance. At the interface

$$p + \frac{1}{2\mu_o} B_{col}^{2} = \frac{1}{2\mu_o} B_{vac}^{2} \qquad (1)$$

where p is the fluid pressure of the plasma column, B_{col} is the strength of the toroidal field in the column, and B_{vac} is the strength of the vacuum magnetic field at the plasma-vacuum interface. The fundamental problem is to determine the shape and location of the interface. An explicit determination is obtained, in terms of elliptic integrals, using conformal mappings. This standard technique, due to Kirchoff[4] for the solution of free boundary problems, was first applied to plasma containment in the study of cusped geometrics,[5] and, more recently, in the determination of the location and shape of the plasma column during an adiabatic tokomak compression.[6] For boundaries which are very high compared to their width ($\frac{H}{R} >> 1$, see Fig. 2), we show, using an asymptotic analysis, that if the ratio, column height/column width is to be large, then the toroidal current used to compress the column can not be too great. Very high compression can only be achieved by a sacrifice of column elongation.

Numerically, we find that an equilibrium plasma column with a compression ratio less than two has dimensions comparable to those of the confining outer boundary. As the compression ratio is increased beyond two, the ratio of plasma height/width decreases to unity. For high compression ratios, the column achieves an essentially circular cross-section. Detailed results are presented in Section IV for $\frac{H}{R} = 5.9$, the dimensions of the belt pinch at the Max Plank Institut für Plasmaphysik at Garching bei Munchen.

II. The Free Boundary Problem

In the vacuum field region, the poloidal field satisfies the equations

$$\nabla \times \vec{B} = 0 \tag{2}$$

$$\nabla \cdot \vec{B} = 0 \quad . \tag{3}$$

These equations imply the existence of a scalar, Φ, not necessarily single-valued, such that in the vacuum region

$$\vec{B} = -\nabla\Phi \tag{4}$$

and

$$\Delta\Phi = 0 \quad . \tag{5}$$

In view of the symmetry, it suffices to determine Φ in the vacuum region contained in $S = \{(x,y) | 0 < x < H,\ 0 < y < R\}$ (see Fig. 3).

For convenience, we introduce normalized variables. We normalize the poloidal field so that its strength is unity at the plasma boundary. We define ψ_0 to be the negative of the ratio of the vacuum poloidal flux to the poloidal field at the plasma-vacuum interface. The normalized poloidal field will be denoted by $\vec{b}$. Its x and y components will be denoted u and v respectively. The normalized potential is $\phi(x,y)$ and its harmonic conjugate (the stream function) is $\psi(x,y)$. Thus

$$\vec{b} = -\nabla\phi \tag{6}$$

$$u = -\phi_x = -\psi_y \tag{7}$$

$$v = -\phi_y = +\psi_x \tag{8}$$

$$\Delta\phi = \Delta\psi = 0 \quad . \tag{9}$$

The boundary conditions which ϕ must satisfy are: (i) on the straight line segments through $y = R$ and $x = H$, $\frac{\partial\phi}{\partial x} = 0$ and $\frac{\partial\phi}{\partial y} = 0$ respectively; (ii) on each of the remaining straight line segments bounding the vacuum field region contained in S, ϕ is constant; (iii) at the interface $|\nabla\phi| = 1$.

It happens that for our normalized potential, there is a one parameter family of solutions. This parameter is ψ_o. The method used to determine ϕ, and, at the same time, the free boundary, is due to Kirchoff[4] and utilizes conformal mapping. Consequently, we introduce the complex variables z, w, and f defined by

$$z = x + iy \tag{10}$$

$$w = u - iv \tag{11}$$

$$f = \phi + i\psi \quad . \tag{12}$$

Assuming the real and imaginary parts of w and f to be twice continuously differentiable functions of x and y, we find w and f to be analytic functions of z. Moreover, from Eqs. (10)-(12)

$$w(z) = -\frac{df}{dz} \quad . \tag{13}$$

Using $f(iA_1) = 0$ (see Fig. 3), we find that z is given parametrically by

$$z = -\int_{0}^{f} \frac{1}{w}\, df + iA_1 \tag{14}$$

$$iR = -\int_{0}^{i\psi_o} \frac{1}{w}\, df + iA_1 \quad . \tag{15}$$

If z is on the free boundary, we have

$$z = -\int_{0}^{\phi} \frac{1}{w}\, df + iA_1 \quad . \tag{16}$$

Thus, the free boundary is determined if w can be determined as an analytic function of f. This is accomplished by a conformal transformation which maps the range of f onto the range of w. These two ranges are shown in Figs. (4) and (5). The mapping of the range of f onto that of w must preserve the correspondence of points of common origin. Thus, using Figs. (3), (4) and (5), we obtain the following table for the mapping. In this table we have defined the number $[\phi]$ as

$$[\phi] = \oint \frac{\partial\phi}{\partial s}\, ds \tag{17}$$

where the integral is taken so that the vacuum field region lies on the left of the path of integration, and the α_i satisfy $0 < \alpha_i < 1$.

z	w	f
iR	$-\alpha_1$	$i\psi_o$
iA_1	-1	0
A_2	$-i$	$\frac{1}{4}[\phi]$
H	$-i\alpha_2$	$\frac{1}{4}[\phi]+i\psi_o$
$H+iR$	0	$\alpha_3\frac{[\phi]}{4} + i\psi_o$

TABLE I

This table determines a unique analytic transformation taking the indicated domain of f onto that of w. In particular, introducing the auxiliary complex variable λ it is possible to write w and f parametrically as the image of the half plane $\operatorname{Im} \lambda > 0$

$$w = - \frac{(-\frac{1}{\lambda})^{1/2}}{\left(\frac{\lambda-1}{\lambda}\right)^{1/2}+1} \tag{18}$$

$$\frac{df}{d\lambda} = +\Gamma(\lambda-\lambda_R)^{-1/2}\lambda^{-1/2}(\lambda-1)^{-1/2}(\lambda-\lambda_H)^{-1/2} \quad . \tag{19}$$

In equation (19) the quantities λ_R and λ_H are the values of λ associated with $z = iR$ and $z = H$ respectively (i.e. $f = i\psi_o$ and $f = \frac{1}{4}[\phi]$ respectively). The numbers $\lambda = 0$ and $\lambda = 1$ have been assigned to $z = iA_1$ and $z = A_2$ respectively (see Fig. 6). The corner $z = H+iR$ has been mapped to infinity in the λ plane.

The quantity Γ is determined by the condition

$$i\psi_o = \int_0^{\lambda_R} \frac{df}{d\lambda}\, d\lambda \qquad . \qquad (20)$$

In equations (18) and (19), square roots are taken with branch cuts along the negative real axis and principle value along the positive real axis.

Equation (18), which maps the range of w onto the half-plane, may be obtained by first mapping the w-domain onto the first quadrant with a rotation, followed by a squaring and a fractional linear transformation. A second squaring covers the half-plane, and a second fractional linear transformation assigns points as described above. Equation (19), mapping f onto the upper half-plane, is obtained using a Schwarz-Christoffel transformation.

Equations (15), (16), (18) and (19) give the shape of the free boundary explicitly as an elliptic integral. Integrals of this type are readily evaluated using standard numerical proceedures. At critical parameters ranges, where numerical calculations are awkward, asymptotic approximations may be found.

III. Asymptotics

After changes of variables in equations (14), (18) and (19), we obtain, writing $\varepsilon \equiv -\lambda_R$ and $1 + \delta \equiv \lambda_H$ ($\varepsilon > 0$, $\delta > 0$)

$$\frac{R}{\psi_o} = \sqrt{2}\;\frac{\displaystyle\int_{-1}^{+1} \frac{d\xi}{\sqrt{1-\xi^2}}\,\frac{1}{\sqrt{2+\frac{\varepsilon}{1+\delta}(1+\xi)}}\left\{\frac{1}{\sqrt{2(1+\delta)}} + \frac{1}{\sqrt{2(1+\delta)-(1+\xi)}}\right\}}{\displaystyle\int_{-1}^{+1} \frac{d\xi}{\sqrt{1-\xi^2}}\,\frac{1}{\sqrt{1+\frac{\varepsilon}{2}(1+\xi)}}\,\frac{1}{\sqrt{2(1+\delta)+\varepsilon(1+\xi)}}} \tag{21}$$

$$\frac{H}{\psi_o} = \sqrt{2}\;\frac{\displaystyle\int_{-1}^{+1} \frac{d\xi}{\sqrt{1-\xi^2}}\,\frac{1}{\sqrt{1+\xi+\frac{2\varepsilon}{1+\delta}}}\left\{\frac{1}{\sqrt{2(1+\delta)}} + \frac{(\varepsilon/1+\delta)^{1/2}}{\sqrt{1+\xi+2\varepsilon}}\right\}}{\displaystyle\int_{-1}^{+1} \frac{d\xi}{\sqrt{1-\xi^2}}\,\frac{1}{\sqrt{1+\frac{\varepsilon}{2}(1+\xi)}}\,\frac{1}{\sqrt{2(1+\delta)+\varepsilon(1+\xi)}}} \tag{22}$$

$$\frac{A_1}{\psi_o} = \frac{\displaystyle\int_{-1}^{+1} \frac{d\xi}{\sqrt{1-\xi}}\,\frac{1}{\sqrt{1+\xi+2\varepsilon}}\,\frac{1}{\sqrt{2(1+\delta)-(1+\xi)}}}{\displaystyle\int_{-1}^{+1} \frac{d\xi}{\sqrt{1-\xi^2}}\,\frac{1}{\sqrt{1+\frac{\varepsilon}{2}(1+\xi)}}\,\frac{1}{\sqrt{2(1+\delta)+\varepsilon(1+\xi)}}} \tag{23}$$

$$\frac{A_2}{\psi_o} = \frac{\displaystyle\int_{-1}^{+1} \frac{d\xi}{\sqrt{1+\xi}}\,\frac{1}{\sqrt{1+\xi+2\varepsilon}}\,\frac{1}{\sqrt{2(1+\delta)-(1+\xi)}}}{\displaystyle\int_{-1}^{+1} \frac{d\xi}{\sqrt{1-\xi^2}}\,\frac{1}{\sqrt{1+\frac{\varepsilon}{2}(1+\xi)}}\,\frac{1}{\sqrt{2(1+\delta)+\varepsilon(1+\xi)}}} \tag{24}$$

We shall assume that the dimensions of the outer boundary, H and R, have been given. Then equations (21) and (22) determine permissible values of ε and δ (i.e. λ_R and λ_H) as functions of ψ_o. Thus, for ψ_o given, equations (14), (18) and (19) determine the free boundary. In particular, equations (23) and (24) give the locations of the extremities of the free boundary. We shall obtain the asymptotic dependence of δ and ε on $\frac{H}{R}$ and ψ_o in the limit $\frac{\varepsilon}{1+\delta} << 1$. The condition $\frac{\varepsilon}{1+\delta} << 1$ is a necessary condition for $\frac{H}{R} >> 1$. This may be seen as follows. From equations (21) and (22), we find

$$\frac{H}{R} = \frac{\displaystyle\int_{-1}^{+1} \frac{d\xi}{\sqrt{1-\xi^2}} \frac{1}{\sqrt{1+\xi+\frac{2\varepsilon}{1+\delta}}} \left\{ \frac{1}{\sqrt{2(1+\delta)}} + \frac{(\varepsilon/1+\delta)^{1/2}}{\sqrt{1+\xi+2\varepsilon}} \right\}}{\displaystyle\int_{-1}^{+1} \frac{d\xi}{\sqrt{1-\xi^2}} \frac{1}{\sqrt{2+\frac{\varepsilon}{1+\delta}(1+\xi)}} \left\{ \frac{1}{\sqrt{2(1+\delta)}} + \frac{1}{\sqrt{2(1+\delta)-(1+\xi)}} \right]} \tag{25}$$

If $\frac{\varepsilon}{1+\delta} >> 1$, the numerator of the right hand side of equation (25) is approximately given by $\frac{\pi}{\sqrt{\varepsilon}}$. The denominator is greater, using crude estimates, than

$$\begin{aligned} &\frac{1}{\sqrt{2\varepsilon}} \int_{-1}^{+1} \frac{d\xi}{\sqrt{1-\xi^2}} \frac{1}{\sqrt{2+\frac{\varepsilon}{1+\delta}(1+\xi)}} \left(\frac{\varepsilon}{1+\delta}\right)^{1/2} \\ &\qquad > \frac{1}{\sqrt{2\varepsilon}} \int_{-1}^{+1} \frac{d\xi}{\sqrt{1-\xi^2}} \frac{1}{\sqrt{3+\xi}} > \frac{\pi}{2^{3/2}\sqrt{\varepsilon}} \end{aligned} \tag{26}$$

so that the right hand side is certainly smaller than $2^{3/2}$. Thus $\frac{\varepsilon}{1+\delta} >> 1$ is incompatible with $\frac{H}{R} >> 1$. If $\frac{\varepsilon}{1+\delta}$ is of order unity, but bounded away from zero, we see that the numerator of the right hand side of equation (25) is of order $\frac{1}{\sqrt{1+\delta}}$ while the denominator is greater than

$$\int_{-1}^{+1} \frac{d\xi}{\sqrt{1-\xi^2}} \frac{1}{\sqrt{2+\frac{\varepsilon}{1+\delta}(1+\xi)}} \frac{1}{\sqrt{2(1+\delta)}} = O\left(\frac{1}{\sqrt{1+\delta}}\right) . \qquad (27)$$

In this event, we again find that $\frac{H}{R}$ can not be much larger than unity. We conclude, therefore, that $\frac{\varepsilon}{1+\delta} << 1$ is a necessary condition for $\frac{H}{R} >> 1$. We now proceed to investigate this limit.

For $\tau \to 0+$ it has been shown[6] that

$$\int_{-1}^{+1} \frac{d\xi}{\sqrt{1-\xi^2}} \frac{1}{\sqrt{1+\xi+\tau}} \sim \frac{1}{\sqrt{2}} \ln \frac{32}{\tau} . \qquad (28)$$

Using equation (28) and $\frac{\varepsilon}{1+\delta} << 1$ we find

$$\pi\frac{H}{R} \sim \frac{\ln 16\frac{1+\delta}{\varepsilon} + 2\varepsilon^{1/2} \int_{-1}^{+1} \frac{d\xi}{\sqrt{1-\xi^2}} \frac{1}{\sqrt{1+\xi+2\varepsilon}} \frac{1}{\sqrt{1+\xi+\frac{2\varepsilon}{1+\delta}}}}{1 + \frac{1}{\pi} \int_{-1}^{+1} \frac{d\xi}{\sqrt{1-\xi^2}} \frac{\sqrt{2(1+\delta)}}{\sqrt{2(1+\delta)-(1+\xi)}}} . \qquad (29)$$

There are four regions in the ε-δ plane in which $\frac{\varepsilon}{1+\delta} << 1$. These are: (i) $\varepsilon << 1$ and $\delta << 1$; (ii) $\varepsilon << 1$ and $\delta = O(1)$; (iii) $\varepsilon << 1$ and $\delta >> 1$; (iv) $\varepsilon \geq \varepsilon_0 > 0$, $\delta >> 1$ and $\varepsilon << \delta$.

For case (i), we easily find, making use of equations (A-1) and (A-7) of the Appendix,

$$\frac{H}{\psi_o} \sim 1 + \frac{1}{\pi} \ln \frac{16}{\varepsilon} \tag{30}$$

$$\frac{R}{\psi_o} \sim 1 + \frac{1}{\pi} \ln \frac{16}{\delta} \tag{31}$$

$$\frac{A_2}{\psi_o} = \frac{1}{\pi} \ln \frac{16}{\varepsilon} \tag{32}$$

$$\frac{A_1}{\psi_o} \sim \frac{1}{\pi} \ln \frac{16}{\delta} \quad . \tag{33}$$

With R held fixed, we see that this limit corresponds to $\psi_o \to 0$. Moreover, in this limit $\frac{A_2}{A_1} \sim \frac{H}{R}$. In section IV we shall show that this limit corresponds to the case where the column occupies nearly all of the interior of the container.

Case (ii) also corresponds to $\frac{A_2}{A_1}$ large. However, $\frac{R}{\psi_o} = O(1)$, so that $\psi_o = O(1)$. This implies that $A_1 = O(1)$ while $A_2 >> 1$. The compression ratio of the column is, therefore, asymptotically given by $\frac{R}{A_1}$

$$\frac{R}{A_1} \sim 1 + \frac{\frac{\pi}{\sqrt{2(1+\delta)}}}{\int_{-1}^{+1} \frac{d\xi}{\sqrt{1-\xi^2}} \frac{1}{\sqrt{2(1+\delta)-(1+\xi)}}} < 2 \tag{34}$$

since $$\frac{\sqrt{2(1+\delta)}}{\sqrt{2(1+\delta)-(1+\xi)}} > 1 \quad \text{for } \xi > -1 \quad .$$

In case (iii) we obtain, using equation (A-9) of the Appendix

$$\frac{H}{\psi_o} \sim \frac{1}{\pi} \ell n \left\{ (16)^2 \frac{(1+\delta)^2}{\varepsilon} \right\} \tag{35}$$

$$\frac{R}{\psi_o} \sim 2 \tag{36}$$

$$\frac{A_2}{\psi_o} \sim \frac{1}{\pi} \ell n \frac{4}{\varepsilon} \tag{37}$$

$$\frac{A_1}{\psi_o} \sim 1 \quad . \tag{38}$$

Moreover, the compression ratio, again asymptotically given by $\frac{R}{A_1}$, is asymptotically

$$\frac{R}{A_1} \sim 2 - \frac{1}{4} \frac{1}{1+\delta} \quad . \tag{39}$$

For case (iv), we find $\frac{A_2}{A_1} = O(1)$. For $\varepsilon >> 1$, $\frac{A_2}{A_1} \sim 1$, with

$$\frac{R}{A_1} \sim \pi \, \varepsilon^{1/2} \tag{40}$$

the column contracts to a nearly circular line source. In particular

$$\frac{H}{\psi_o} \sim \frac{2\varepsilon^{1/2} \ \ell n \ 16 \ \frac{1+\delta}{\varepsilon}}{\ell n \ 16\varepsilon} \tag{41}$$

$$\frac{R}{\psi_o} \sim \frac{2\pi \ \varepsilon^{1/2}}{\ell n \ 16\delta} \tag{42}$$

$$\frac{A_2}{\psi_o} \sim \frac{2}{\ell n \ 16\varepsilon} \tag{43}$$

$$\frac{A_1}{\psi_o} \sim \frac{2}{\ell n \ 16\delta} \quad . \tag{44}$$

Formulas (30) and (31) may be combined to give an asymptotic estimate of δ in terms of $\frac{H}{R}$ and ε. For $\varepsilon < \delta < .001$, the agreement of the estimate with the exact value of δ is better than 1%. Similar results are found using equations (35) and (36) with $\varepsilon < .01$ and $\delta > 1000$, and using equations (41) and (42) with $\varepsilon > 100$ and $\delta > 100\varepsilon$. Referring to Fig.7 , we see that the above regions in which the asymptotic formulas are accurate cover a substantial portion of the figure. The level contours of $\frac{H}{R}$ were computed using equation (25).

The asymptotic expressions for $\frac{H}{\psi_o}$ and $\frac{R}{\psi_o}$ determine relations between $1+\delta$ and ε which depend only on the ratio $\frac{H}{R}$. Thus, in case (i) and in case (iv) with $\varepsilon >> 1$, we obtain

$$1 + \delta \sim 1 + \varepsilon^{R/H}(16e^{\pi})^{(1- R/H)} \tag{45}$$

$$1 + \delta \sim \frac{\varepsilon}{16}\, e^{(\pi\ H/R)} \tag{46}$$

respectively. These formulas, together with equations (31) and (42) may be used to solve for ε and $1+\delta$ as functions of ψ_o yielding equations (47) and (49). Using these functions of ψ_o we obtain equations (48) and (50) below. Thus, for case (i)

$$1 + \delta \sim 1 + 16e^{-\pi(\frac{R}{\psi_o} -1)} \quad ; \qquad \varepsilon \sim 16e^{-(\frac{H}{R}\frac{R}{\psi_o} -1)} \tag{47}$$

$$\begin{aligned} A_1 &\sim \psi_o(\frac{R}{\psi_o} -1) \\ A_2 &\sim \psi_o(\frac{H}{R}\frac{R}{\psi_o} -1) \end{aligned} \tag{48}$$

while for case (iv)

$$1 + \delta \sim 1 + (16e^{\pi})^{(1-R/H)}\{\frac{1}{\pi}\,\frac{R}{\psi_o}\,\ell n\,(\frac{4}{\pi}\,\frac{R}{\psi_o})\}^{(2R/H)};$$

$$\varepsilon^{1/2} \sim \frac{1}{\pi}\,\frac{R}{\psi_o}\,\ell n\,\frac{4}{\pi}\,\frac{R}{\psi_o} \qquad (49)$$

$$A_1 \sim \psi_o\,\frac{1}{\ell n\,\frac{4}{\pi}\,\frac{R}{\psi_o}}$$

$$A_2 \sim \psi_o\,\frac{1}{\ell n\,\frac{4}{\pi}\,\frac{R}{\psi_o}}\,. \qquad (50)$$

In both cases, the formulae are valid for the limit $\psi_o \to 0$.

With ε and $1+\delta$ (i.e. $-\lambda_R$ and λ_H) determined as functions of ψ_o, the free boundary is determined as a function of the single parameter ψ_o.

IV. Adiabatic Compression

We now consider an adiabatic compression of the plasma by a toroidal discharge at the outer conductor. We shall assume that the poloidal field (i.e. the field in the plane of Fig. 2) vanishes in the region outside the outer boundary. With this assumption, if I is the magnitude of the total toroidal current flowing at the outer boundary and B_i is the poloidal field strength at the interface, then

$$I = \frac{B_i}{\mu_o} L \tag{51}$$

where L is the length of the perimeter of the curve bounding the interface in the plane of Fig. 2. For simplicity, we shall assume that compression is begun with a column filling the container. The initial strength of the toroidal field trapped in the perfectly conducting column will be given by B^*_{col}. Its strength at any other time will be indicated by B_{col}. The flux of this field is conserved during compression. Therefore, if A is the cross-sectional area at some later time

$$B_{col}\, A = B^*_{col}\,(4HR) \quad . \tag{52}$$

The compression ratio of the column, C, is then given by

$$C = \frac{4HR}{A} \quad . \tag{53}$$

During compression, the plasma mass is also conserved, so that the density, ρ, initially given by ρ^*, satisfies

$$\rho A = \rho^*(4HR) \quad . \tag{54}$$

Assuming the compression to be isentropic, the plasma pressure, p, and temperature, T, are computed from

$$p = \mathcal{A}\,\rho^{\gamma} \qquad (55)$$

$$T = \mathcal{A}'\,\rho^{\gamma-1} \qquad (56)$$

where $\mathcal{A}$, $\mathcal{A}'$ and γ are constants ($\mathcal{A}' = \frac{\mathcal{A}}{\kappa}$ where $p = \rho\kappa T$). It is convenient, in place of the pressure, p, to define a column pressure, p_{col}, for the plasma

$$p_{col} = p + \frac{1}{2\mu_o} B^2_{col} \quad . \qquad (57)$$

The initial value of the total toroidal current flowing at the outer boundary, I^*, is given by

$$I^* = \frac{4H+4R}{\mu_o} \sqrt{2\mu_o p^*_{col}} = \frac{4H+4R}{\mu_o} \sqrt{2\mu_o \left(p^* + \frac{1}{2\mu_o} B^{*2}_{col}\right)} \quad .$$

From equation (1)

$$I = \frac{\sqrt{2\mu_o p_{col}}}{\mu_o} L \quad . \qquad (58)$$

Since p_{col} depends only on the initial data and compression ratio C of the column and since C and the length, L, depend only on ψ_o, the value of ψ_o determines I. The relationship between ψ_o and I must be found numerically. However, for some limiting configurations of special interest, simple asymptotic relations are readily obtained.

If the height of the column, $2A_2$, satisfies $2A_2/2H \approx 1$, the poloidal curvature is negligible near the toroidal midplane, $L/4H \approx 1$, $C \approx R/A_1$, and $\psi_o \approx R-A_1$. For $\gamma = 2$, we find

$$\frac{I}{I^*} \sim \frac{R}{A_1} \tag{59}$$

Using equation (48) we obtain, for $\psi_o/R << 1$,

$$\frac{I}{I^*} \sim \frac{\frac{R}{\psi_o}}{\frac{R}{\psi_o} - 1} \; ; \quad \frac{R}{\psi_o} \sim \frac{\frac{I}{I^*}}{\frac{I}{I^*} - 1} \tag{60}$$

From equations (34), (36), (38) and (59), we find that maximum compression ratios for a column with high eccentricity are obtained when $I/I^* \approx 2$.

In order to obtain the relationship between I and ψ_o as the column cross-section becomes small, we first obtain the approximate poloidal field at the toroidal midplane. For a rectangular outer boundary, this can be done using the method of images. In particular, if $H/R >> 1$, we may neglect end effects. Replacing the column by a line source, image sources of equal strength and alternating direction are added at $y=\pm 2nR$ (see Fig. 8) yielding a field which is tangent to the outer boundary at $y=\pm R$. On the y-axis (the toroidal midplane), the poloidal field due to the image sources, assuming unit current in the column is

$$\frac{\mu_o}{2\pi} \left\{ \sum_{n=1}^{\infty} (-1)^n \frac{-2y}{4n^2R^2-y^2} \right\} \tag{61}$$

The associated poloidal flux is given by

$$\frac{\mu_o}{2\pi} \ln \prod_{n=1}^{\infty} \left(\frac{4n^2-1}{4n^2} \right)^{(-1)^n} = \frac{\mu_o}{2\pi} \ln \frac{4}{\pi} \qquad (62)$$

In obtaining Eq. (62) the true dimensions of the column have been neglected.

If the column has a cross-section which is approximately circular with radius A_1, then the poloidal flux due to the column is $\frac{\mu_o}{2\pi} \ln \frac{R}{A_1}$. If the toroidal current flowing in the outer conductor, and hence the column, is I, (initially given by $I^* \sim \frac{4H}{\mu_o} \sqrt{2\mu_o p^*_{col}}$), then the poloidal flux through the y-axis is asymptotically given by

$$\psi \sim \mu_o \frac{I}{2\pi} \ln \frac{4}{\pi} \frac{R}{A_1} \quad . \qquad (63)$$

For $\gamma = 2$, using equation (50), and $A \sim \pi A_1^2$, we obtain

$$\frac{R}{\psi_o} \sim \frac{1}{2} \frac{\left(\frac{I}{I^*}\right)}{\ln \left(\frac{I}{I^*}\right)} \quad ; \quad \frac{I}{I^*} \sim 2 \frac{R}{\psi_o} \ln \frac{R}{\psi_o} \quad . \qquad (64)$$

Using equations (60) and (64) we obtain the following table for the asymptotic variation of the indicated thermodynamic parameters of the system in terms of the toroidal current flowing at the outer boundary. Figure 9 shows the numerically obtained dependence of the compression ratio on this toroidal current when $\frac{H}{R} = 5.9$. The asymptotic estimates of the compression ratio given in Table II are also shown.

$\gamma = 2$	$C \equiv \frac{\rho}{\rho^*} = \frac{T}{T^*}$	$\frac{p}{p^*}$	$\frac{A_2}{A_1}$
$\frac{I}{I^*} \sim 1$	$(\frac{I}{I^*})^{(1+2R/H)}$	$(\frac{I}{I^*})^{2(1+2R/H)}$	$(1- \frac{I}{I^*}) + \frac{H}{R} \frac{I}{I^*}$
$\frac{I}{I^*} >> 1$	$\frac{H/R}{\pi} (\frac{I}{I^*})^2$	$(\frac{H/R}{\pi})^2 (\frac{I}{I^*})^4$	1

TABLE II

As seen in figure 9 the compression may be divided into three stages. Near the onset of compression, I/I^* less than 1.6, the column maintains a shape comparable to that of the outer boundary. For the intermediate compression region, with compression ratio between 2.5 and 10, the width of the column remains nearly constant but its height diminishes rapidly as I/I^* is increased. In the third stage of compression the plasma cross-section is circular and very high compression ratios are obtained. Plasma cross-sections representative of these stages are shown in figure 10.

Acknowledgment

The authors wish to thank Dr. W. Grossmann for many informative discussions.

Appendix

In this section, we derive the asymptotic dependence of the numerator of equation (25). The relation[6]

$$\int_{-1}^{+1} \frac{d\xi}{\sqrt{1-\xi^2}} \frac{1}{\sqrt{1+\xi+\tau}} \sim \frac{1}{\sqrt{2}} \ln \frac{32}{\tau} \qquad \text{(A-1)}$$

valid for $\tau \to 0+$ will be used. Employing equation (A-1), the first integral, I_1, in the numerator of equation (25) is asymptotically given by

$$I_1 \sim \frac{1}{\sqrt{2(1+\delta)}} \frac{1}{\sqrt{2}} \ln\left\{16 \frac{1+\delta}{\varepsilon}\right\} \qquad \text{(A-2)}$$

In order to obtain the asymptotic expansion for the second integral, I_2, we introduce the notation $\bar{\varepsilon} = 2\varepsilon$, $\underline{\varepsilon} = \frac{2\varepsilon}{1+\delta}$.

$$I_2 = \frac{1}{\sqrt{2(1+\delta)}} \bar{\varepsilon}^{1/2} \int_{-1}^{+1} \frac{d\xi}{\sqrt{1-\xi^2}} \frac{1}{\sqrt{1+\xi+\bar{\varepsilon}}} \frac{1}{\sqrt{1+\xi+\underline{\varepsilon}}} \qquad \text{(A-3)}$$

The integral in equation (A-3) may be written as

$$\int_0^2 \frac{dy}{y^{1/2}\sqrt{2-y}} \frac{1}{\sqrt{y+\bar{\varepsilon}}\,\sqrt{y+\underline{\varepsilon}}} = \int_0^s + \int_s^2 \frac{dy}{y^{1/2}\sqrt{2-y}} \frac{1}{\sqrt{y+\bar{\varepsilon}}} \frac{1}{\sqrt{y+\underline{\varepsilon}}} \qquad \text{(A-4)}$$

where s is to be taken "small" as prescribed below. If s is chosen so that $\bar{\varepsilon}/s \to 0$, we find

$$\bar{\varepsilon}^{1/2} \int_s^2 \frac{dy}{y^{1/2}\sqrt{2-y}} \, \frac{1}{\sqrt{y+\bar{\varepsilon}}} \, \frac{1}{\sqrt{y+\underline{\varepsilon}}} \sim \bar{\varepsilon}^{1/2} \int_s^2 \frac{dy}{y^{3/2}\sqrt{2-y}}$$

$$= \bar{\varepsilon}^{1/2} \left(- \frac{\sqrt{2-y}}{y^{1/2}} \right) \Bigg|_s^2 \sim \left(\frac{\bar{\varepsilon}}{s}\right)^{1/2} \sqrt{2} \qquad \text{(A-5)}$$

which goes to zero with $\frac{\bar{\varepsilon}}{s}$. Therefore, up to terms which go to zero with ε,

$$I_2 \sim \frac{1}{\sqrt{2(1+\delta)}} \bar{\varepsilon}^{1/2} \int_0^s \frac{dy}{y^{1/2}\sqrt{2-y}} \, \frac{1}{\sqrt{y+\bar{\varepsilon}}} \, \frac{1}{\sqrt{y+\underline{\varepsilon}}}$$

$$\sim \frac{1}{\sqrt{2(1+\delta)}} \, \frac{\bar{\varepsilon}^{1/2}}{\sqrt{2}} \int_0^s \frac{dy}{y^{1/2}\sqrt{y+\bar{\varepsilon}}} \, \frac{1}{\sqrt{y+\underline{\varepsilon}}} \qquad \text{(A-6)}$$

The change of variables $y = \bar{\varepsilon}\nu$ yields

$$I_2 \sim \frac{1/\sqrt{2}}{\sqrt{2(1+\delta)}} \int_0^{s/\bar{\varepsilon}} \frac{d\nu}{\nu^{1/2}(\nu+1)^{1/2}(\nu+\underline{\varepsilon}/\bar{\varepsilon})^{1/2}}$$

$$\sim \frac{1/\sqrt{2}}{\sqrt{2(1+\delta)}} \int_0^{\infty} \frac{d\nu}{\nu^{1/2}(\nu+1)^{1/2}(\nu+\underline{\varepsilon}/\underline{\varepsilon})^{1/2}}$$

$$= \frac{1/\sqrt{2}}{\sqrt{2(1+\delta)}} \int_{-1}^{-\,\underline{\varepsilon}/\bar{\varepsilon}} \frac{d\nu}{|\nu|^{1/2}|\nu+1|^{1/2}|\nu+\underline{\varepsilon}/\underline{\varepsilon}|^{1/2}}$$

$$= \frac{1/\sqrt{2(1+\delta)}}{\sqrt{\frac{|1-\,\underline{\varepsilon}/\bar{\varepsilon}|}{2}}} \; \frac{1}{\sqrt{2}} \int_{-1}^{+1} \frac{d\rho}{\sqrt{1-\rho^2}\;\sqrt{1+\rho+\frac{2\underline{\varepsilon}/\bar{\varepsilon}}{1-\,\underline{\varepsilon}/\bar{\varepsilon}}}} \qquad \text{(A-7)}$$

If $\psi_o \neq 0$, equation (21) implies $\delta \neq 0$, so that $\underline{\varepsilon}/\bar{\varepsilon} \neq 1$. In the limit $1 + \delta \to \infty$, equation (A-1) yields

$$I_2 \sim \frac{1}{\sqrt{2(1+\delta)}} \; \frac{1}{\sqrt{2}} \; \ell n \; 16(1+\delta) \qquad \text{(A-8)}$$

In this limit, the denominator of equation (25) is easily seen to be asymptotic to $\frac{\pi}{\sqrt{1+\delta}}$. Thus,

$$\frac{H}{R} \sim \frac{1}{2\pi} \; \ell n \; (16)^2 \; \frac{(1+\delta)^2}{\varepsilon} \qquad \text{(A-9)}$$

References

1. Mukhovatov, V.S. and Shafranov, V.D. Nuclear Fusion, 11, (1971) p. 605.
2. Bateman, G., Grossmann, W., von Hagenow, K.U., Lackner, K., private communication.
3. Kadish, A. Nuclear Fusion 15, 5, October, 1973, p. 756.
4. Kirchoff, G. Zur Theorie Freier Flussigkeitsstrahlen, Crelle, 1869.
5. Berkowitz, J., Friedrichs, K.O., Goertzel, H., Grad, H., Killeen, J., and Rubin, E. 2nd Inter. Conf. on Peaceful Uses of Atomic Energy (Proc. Conf. Geneva, 1958), 31, UN, New York (1958) p. 171.
6. Grad, H., Kadish, A., and Stevens, D.C., to appear in Comm. Pure and Applied Math., 1974.

FIG. 1

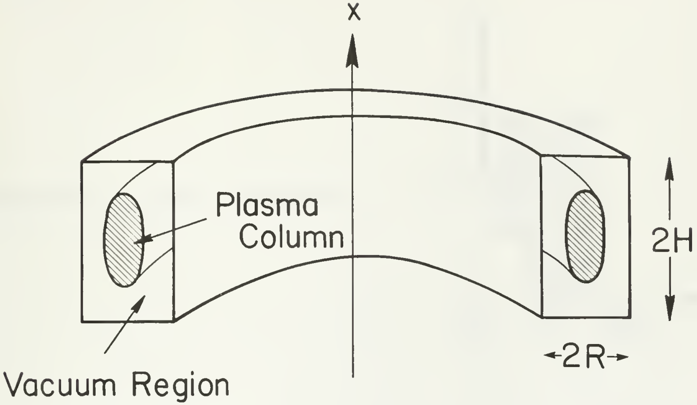
x
Plasma Column
2H
2R
Vacuum Region

FIG. 2

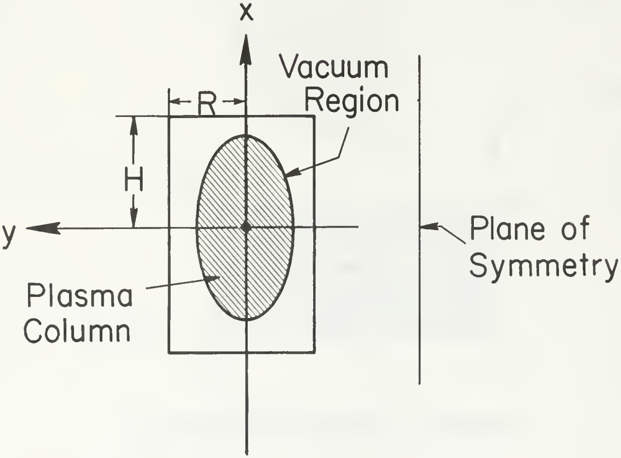
x
Vacuum Region
R
H
y
Plane of Symmetry
Plasma Column

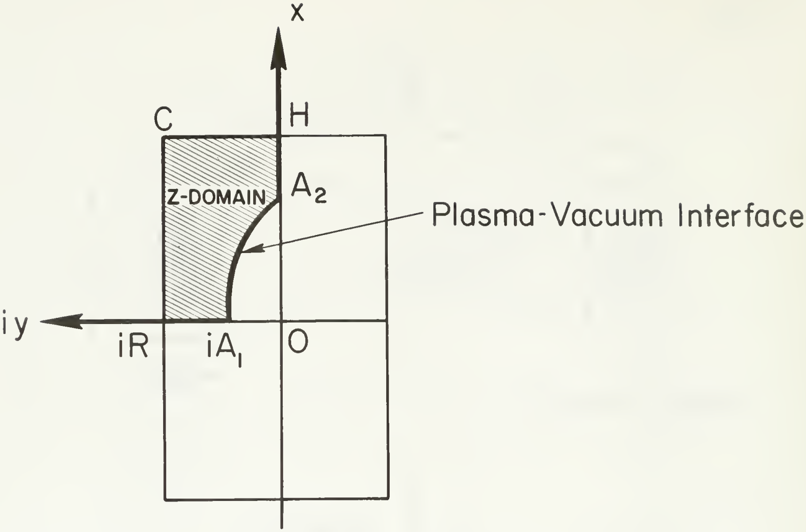
x
C
H
A₂
Z-DOMAIN
Plasma-Vacuum Interface
iy
iR
iA₁
O

FIG. 3

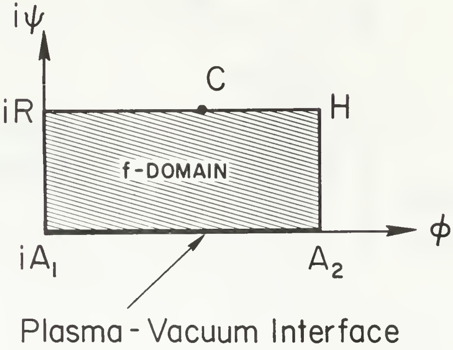
iψ
C
iR
H
f-DOMAIN
φ
iA₁
A₂
Plasma-Vacuum Interface

FIG. 4

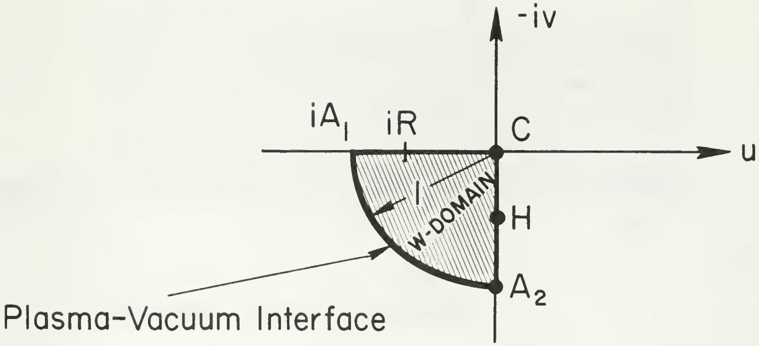

FIG. 5

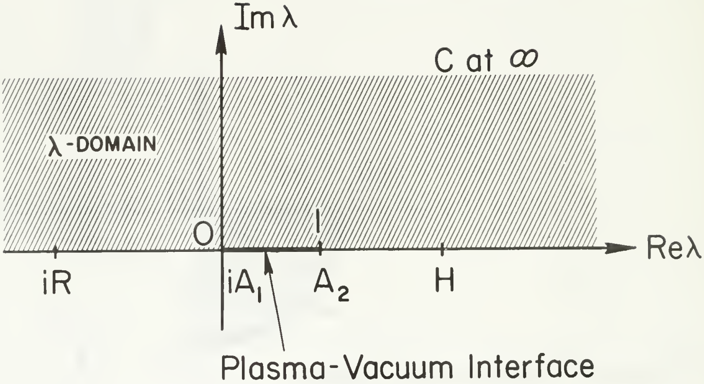

FIG. 6

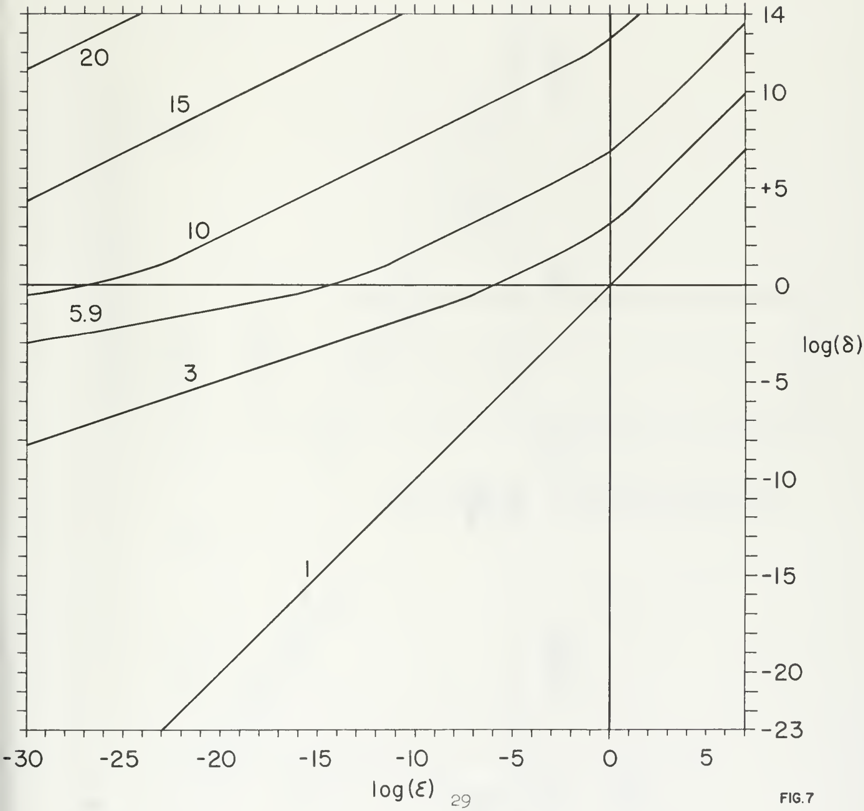

FIG.7

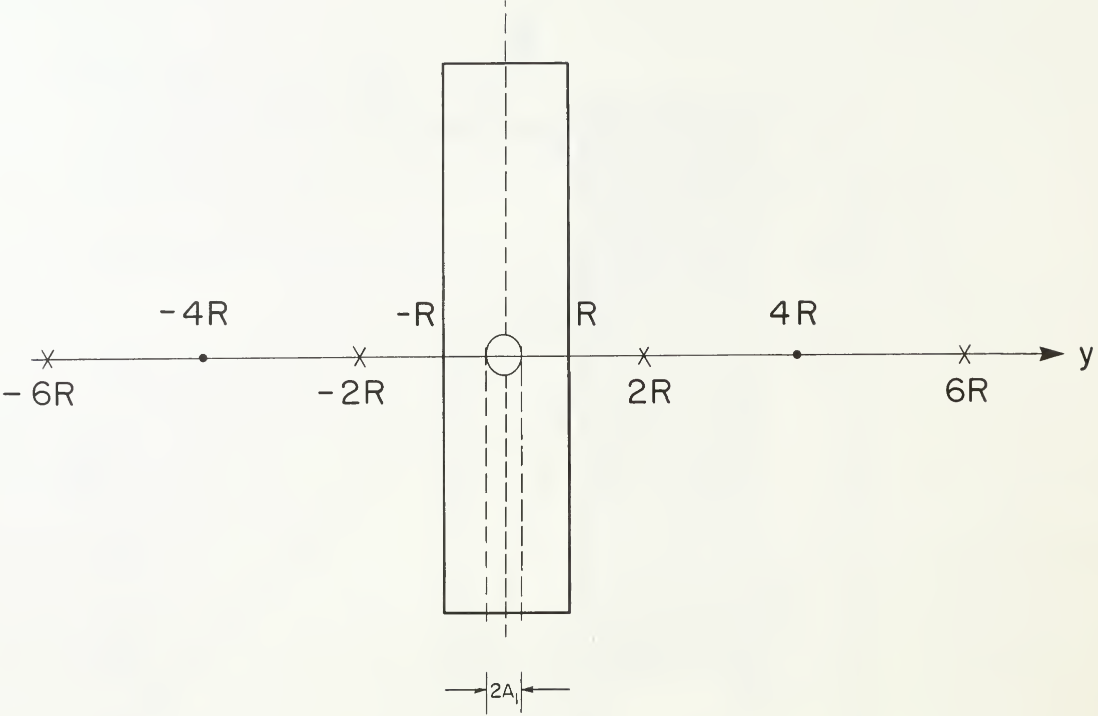

FIG. 8

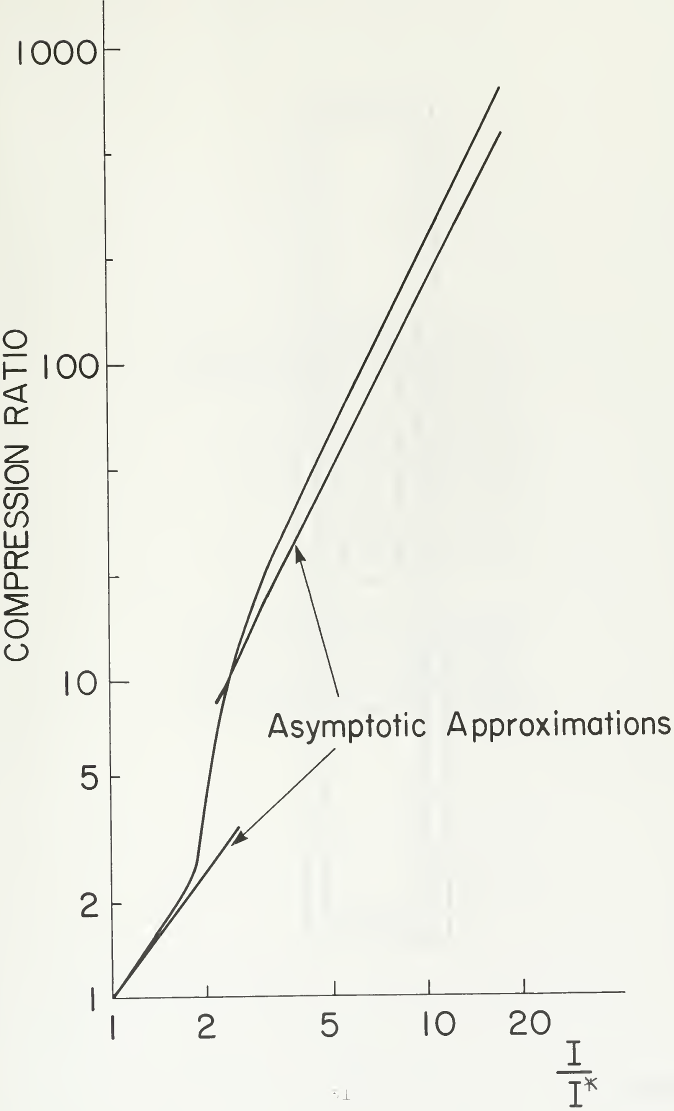
1000
100
10
5
2
1
COMPRESSION RATIO
1
2
5
10
20
I/I*
Asymptotic Approximations

FIG. 9

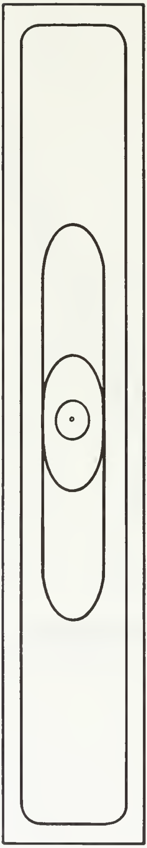

FIG. 10

This report was prepared as an account of Government sponsored work. Neither the United States, nor the Commission, nor any person acting on behalf of the Commission:

A. Makes any warranty or representation, express or implied, with respect to the accuracy, completeness, or usefulness of the information contained in this report, or that the use of any information, apparatus, method, or process disclosed in this report may not infringe privately owned rights; or

B. Assumes any liabilities with respect to the use of, or for damages resulting from the use of any information, apparatus, method, or process disclosed in this report.

As used in the above, "person acting on behalf of the Commission" includes any employee or contractor of the Commission, or employee of such contractor, to the extent that such employee or contractor of the Commission, or employee of such contractor prepares, disseminates, or provides access to, any information pursuant to his employment or contract with the Commission, or his employment with such contractor.